Int. J.Nano Dimens. 6(1): 83-88, Winter 2015
ISSN: 2008-8868

Contents list available at **IJND**

International Journal of Nano Dimension

Journal homepage: *www.IJND.ir*

Ion exchange growth of Zinc Sulfide quantum dots in aqueous solution

A. Pourahmad*

Department of Chemistry, Guilan Science and Research Branch, Islamic Azad University, Guilan, Iran.

Received 31 July 2013
Accepted 28 October 2013

ABSTRACT

We report the growth by ion exchange synthesis of ZnS nanoparticles in MCM-41 matrices using Zn $(CH_3COO)_2$ and Na_2S starting sources. The final product (ZnS/MCM-41) was characterized by X-ray diffraction (XRD) pattern, transmission electron microscopy (TEM), scanning electron microscopy (SEM), infrared spectrometry (IR) and UV-vis spectroscopy. Its crystalline structure and morphology was studied by XRD and scanning electron microscopy. Exciton absorption peaks at higher energy than the fundamental absorption edge of bulk ZnS indicates quantum confinement effects in nanoparticles as a consequence of their small size.

Keywords: *Quantum dots; Semiconductors; Chemical synthesis; Scanning electron microscopy (SEM); Transmission electron microscopy (TEM).*

INTRODUCTION

Nanostructured materials have attracted a great deal of attention in the last few years due to their unique properties that are different from the bulk materials. Zinc sulfide (ZnS) as an important wide-bandgap (3.6 eV) semiconductor has been used as a key material for the ultraviolet light emitting diodes and injection lasers, flat panel displays, electroluminescent devices and infrared windows. In recent years, some characteristics of ZnS nanocrystals different from bulk crystal have enlarged the range of application. Thus, the study of ZnS nanostructure is of considerable importance and great efforts have been focused on the synthesis and physical properties [1-5].

One of the most interesting materials for applications and fundamental investigations are mesoporous material sieves. Since their discovery more one decade ago mesoporous MCM-41 molecular sieve materials have triggered widespread interest in many research fields because of their unique structural and chemical properties [6]. This class of silica tube-like materials features extremely large specific surface areas exceeding 1000 $m^2 g^{-1}$.

* Corresponding author:
Afshin Pourahmad
Department of Chemistry, Guilan Science and Research Branch, Islamic Azad University, Guilan, Iran.
Tel +98 911 3332448
Fax +98 131 7220721
Email pourahmad@iaurasht.ac.ir

The molecular sieves possess uniformly sized mesoporous whose diameter can be controlled between 1.5 and 8 nm by the synthesis conditions chosen and template used. Whereas the mesoporous of MCM-41 are arranged in a regular hexagonal array, the silicon dioxide forming the walls around these tubes shows an amorphous structure. MCM-41 materials have especially attracted interest in adsorptive and catalytic applications involving large molecules. Other promising applications are the use of MCM-41 as hosts for semiconducting and ferroelectric nanomaterials as well as for the study of confined liquids and polymers [7, 8]. In this work we report the synthesis and characterization of MCM-41 materials loaded with zinc sulfide (ZnS) by an ion exchange technique. The results obtained from X-ray, UV-Vis, SEM, TEM experiments are reported.

EXPERIMENTAL

Nano-sized mesoporous MCM-41 silica with particle size ~ 90 nm was synthesized by a room temperature method with some modification to the procedure described in the literature [9]. We used tetraethylorthosilicate (TEOS: Merck, 800658) as a source of silicon and hexadecyltrimethylammonium bromide (HDTMABr; BOH, 103912) as a surfactant template for preparation of the mesoporous material. The molar composition of the reactant mixture is as follows:

TEOS: 0.31NaOH: 0.125HDTMABr: 1197H_2O

The prepared nano-sized MCM-41 was calcined at 550 °C for 5h to decompose the surfactant and obtain the white powder. Surfactant-free MCM-41 nanoparticles were used for loading the zinc sulfide nanoparticles.

As a precursor of ZnS semiconductors, solution of Zn $(CH_3COO)_2$ (0.1 mol l^{-1}) was prepared. To 50 ml of Zn $(CH_3COO)_2$ solution, 1 g of MCM-41 powder was added and the mixture stirred for 12 h at 25 ºC. The sample was then washed to remove nonexchanged Zn^{2+} and air-dried. Finally, sulphurizing of the Zn^{2+} ions was carried out with 0.1 M Na_2S solution. To make the reaction with the S^{2-} ion, one g Zn^{2+} - exchanged zeolite was added to 50 mL of 0.1 M solution of Na_2S at a fixed temperature and magnetically stirred for 2 h. Samples were washed with deionized water and collected by filtration. The obtained samples were in fine white colored powder form. The samples were stable at ambient condition and their color did not change when exposed to atmospheric moisture. The ZnS particles prepared from MCM-41 are described as ZnS/MCM-41, in subsequent discussions.

X-ray diffraction (XRD) pattern was recorded on a Seisert Argon 3003 PTC using nickel-filtered XD-3a CuKα radiations (λ = 1.5418 ºA). The UV-vis diffused reflectance spectra (UV-vis DRS) were obtained from UV-vis Scinco 4100 spectrometer with an integrating sphere reflectance accessory. $BaSO_4$ was used as a reference material. UV-vis absorption spectra were recorded using a Shimadzu 1600 pc in the spectral range of 190-900nm. Transmission electron microscopy (TEM) was performed on a Philips CM10 and microscope operated at 100 kV. Samples were prepared by dispersing the powder in ethanol. Imaging was enabled by depositing few drops of suspension on a carbon coated 400 mesh Cu grid. The solvent was left to evaporate before imaging. Scanning electron microscopy (SEM) images of fabricated ZnS nanoparticles were obtained using LEO 440i electron microscope. The specific surface area and pore volume of the samples were calculated according to the Brunauer-Emmett-Teller (BET) method. Infrared spectra on KBr pellet were measured on a Bruek spectrophotometer.

RESULTS AND DISCUSSION

Figure 1(a and b) shows the XRD patterns of MCM-41 template and ZnS loading on the template. Measurements of the samples were carried out in different 2θ ranges (2θ = 2-10º and 2θ = 20-60º), in the condition of 40 kV and 40 mA, at a step size of 2θ = 0.02º. Low angle X-ray diffraction patterns (2θ = 2-10º) of calcined MCM-41 nanoparticles and ZnS/MCM-41 clearly exhibit four well-defined peaks which can be indexed with (100), (110), (200), and (210) planes on hexagonal unit cell, indicating mesoporous structure of MCM-41. The peak appearing at low angle (2θ = 2.2) corresponds to (100) plane of MCM-41 indicating

ordered pore structure of MCM-41, which can be attributed to quasi-two dimensional hexagonal lattice of MCM-41 [6, 9].

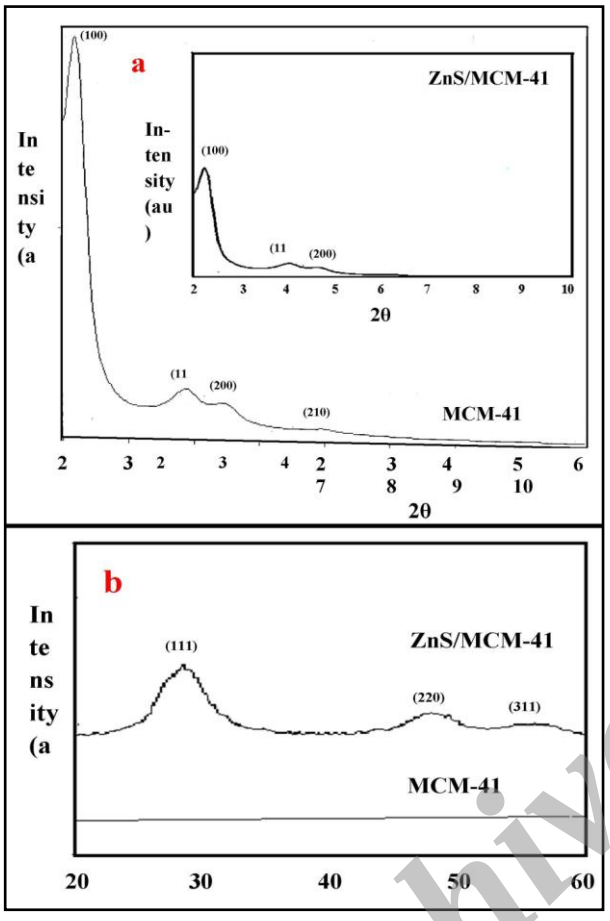

Fig. 1. (a) X-ray diffraction patterns of MCM-41 and ZnS/MCM-41 in range 2θ = 2-10º and (b) X-ray diffraction patterns of MCM-41 and ZnS/MCM-41 in range 2θ = 20-60º.

In this figure, we observed that all X-ray patterns are very similar. However, some differences, such as the broadening and slight shifting to higher angles of the diffraction peaks as well as the decrease of their intensity can be observed in the spectra. This should be attributed to the porefilling effects that can reduce the scattering contrast between the pores and the framework MCM-41 materials. These decreases of the peak intensities, are in agreement with the reported results for other zeolites [10- 12]. High angle X-ray diffraction pattern (2θ = 20-60), Figure 1, further supports presence of ZnS. The diffraction peaks located at (2θ = 28.5), (2θ = 47.7) and (2θ = 56.3), coincide with those of β -ZnS (111), (220), and (311), respectively. This means that ZnS crystals prepared in this study have zinc blended structure. We have determined the size of nanoparticles at the mentioned 2θ by using the Debye-Scherrer formula, $d=0.9\ \lambda/\beta\cos\theta$, where d is the average diameter of the crystalline, λ the wavelength of X-ray, β the excess line width of the diffraction peak in radians and θ the Bragg angle. Based on this analysis the average size of ZnS nanoparticles has been found to be 4 nm (Table 1).

Table 1. Band gap, specific surface area, particle size, pore volume and absorption edge of samples.

Sample	MCM-41	Bulk ZnS	ZnS/MCM-41
Band gap (eV)	-	3.6	4.04
Specific surface area (m^2/g)	850	-	730
Particle size (nm)	90	-	4
Pore volume (cc/g)	1.05	-	0.89
Absorption edge (nm)	-	375	345

The surface morphology of MCM-41 nanoparticles and ZnS/MCM-41 is investigated by SEM and the micrographs are presented in Figure 2. Figure 2 (a) shows the SEM image of MCM-41 nanoparticles where small spherical particles of nanomesoporous silica MCM-41 with diameters of ~ 90 nm are evident. There is no considerable change in morphology of ZnS/MCM-41 (Figure 2 (b)).

The UV-vis diffused reflectance spectra (UV-vis DRS) for ZnS nanoparticles prepared from MCM-41 matrices, bulk ZnS are shown in Figure 3. Bulk ZnS gave absorption below 400 nm. Comparing the absorption edge of bulk ZnS to that of ZnS/MCM-41 sample prepared from mesoporous materials, it is seen that a blue shift in the onset of absorption has occurred in this sample. This blue shift indicates that ZnS exists as small clusters within the zeolite pores as reported by several researchers [13, 14]. This was supported by a significant decrease in the surface area of

ZnS/MCM-41, compared to the parent zeolite (Table 1). This phenomenon of blue shift of absorption edge has been ascribed to a decrease in particle size. It is well known that in case of semiconductors the band gap between the valence and conduction band increases as the size of the particle decreases in the nanosize range. This results in a shift in the absorption edge to a lower wavelength region. The magnitude of the shift depends on the particle size of the semiconductor. In present study, the ZnS/MCM-41 samples prepared from the MCM-41 matrix showed a blue shift of approximately 30 nm compared to the bulk particles. From the onset of the absorption edge, the band gap of the ZnS particles was calculated using the method of Tandon and Gupta [15] (Table 1). The size of ZnS nanoparticles, estimated based on the results of Weller et al. [16] was 4 nm for ZnS/MCM-41 sample.

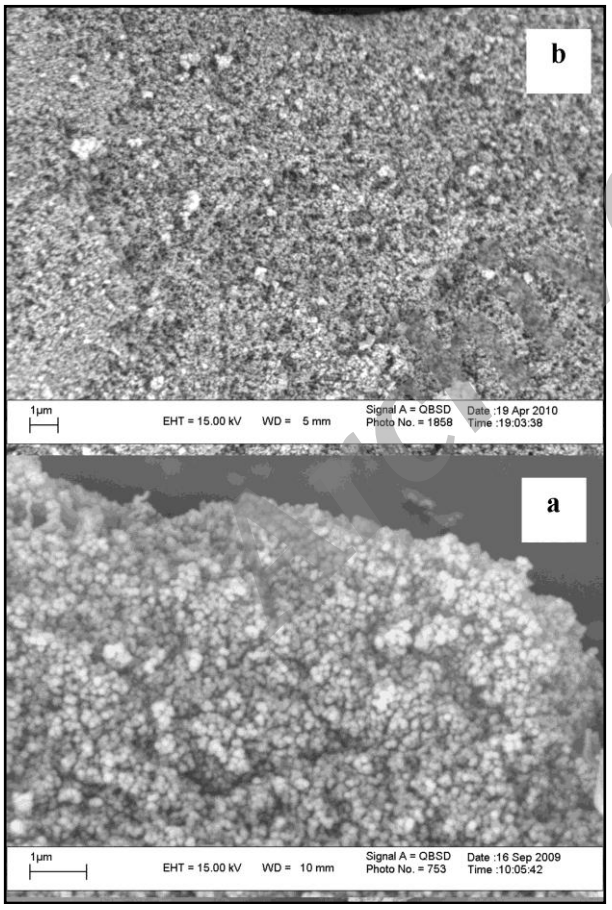

Fig. 2. Scanning electron microscopy (SEM) micrographs of (a) MCM-41 and (b) ZnS/MCM-41.

The results of the specific surface area and pore volume measurements (BET measurements) for MCM-41 and ZnS/MCM-41, show that the pore volume of the host mesoporous material, which was 1.05 ml g^{-1} for MCM-41, decreased to 0.89 ml g^{-1} for ZnS/MCM-41materials. Similarly, the specific surface area of the composite materials was decreased from 850 m^2 g^{-1} for MCM-41 to 730 m^2 g^{-1} for ZnS/MCM-41. Decreasing in the volume of the pores and the specific surface area of the mesoporous material demonstrates that the guests are located in the channels (Table 1).

The IR spectra of MCM-41 and ZnS/MCM-41 samples are recorded in the range of 400-4000 cm^{-1}. The broad absorption band in the region 3765-3055 cm^{-1} can be attributed to the stretching of the framework Si-OH group with the defective sites and physically adsorbed water molecules. The vibrations of Si-O-Si can be seen at 1091 cm^{-1} (asymmetric stretching), 805 cm^{-1} (symmetric stretching) and 454 cm^{-1} (bending) [17, 18]. In present work, all bands in ZnS/MCM-41 sample show shift to higher wave numbers with respect to the MCM-41 zeolite. This shift reveals that nanoparticles could incorporate in MCM-41 zeolite. The increased intensity is observed in nanoparticle sample with respect to MCM-41 zeolite. This increase relates to extent of perturbation of T-O-T vibrations of the zeolite lattice (bands 400-1700 cm^{-1}) and increase in acidic bridged hydroxyls vibrations (3423 cm-1 band) [19,20]. These kinds of differences are related to presence of ZnS nanoparticles in MCM-41.

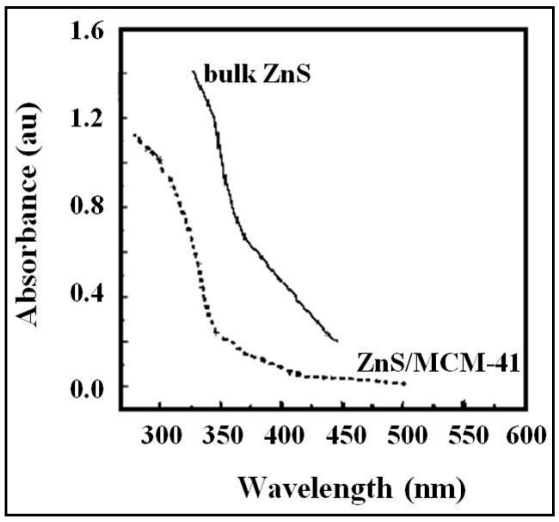

Fig. 3. UV-vis absorption spectrum of bulk ZnS and ZnS/MCM-41.

Transmission electron microscopy along with the textural properties of the samples discussed above bring us important information regarding whether the ZnS particles are located inside or outside the pore structures used in this work. TEM image of ZnS/MCM-41 sample is shown in Figure 4. It was recorded under parallel direction to the pore axis and it is possible to observe typical MCM-41 morphology in the micrograph. Although it is very difficult to identify ZnS nanoparticles within the pores of MCM-41 materials by using TEM techniques [20], the higher contrast in the image of the ZnS/MCM-41 sample can be associated with the presence of ZnS nanoparticles inside the pores of this sample.

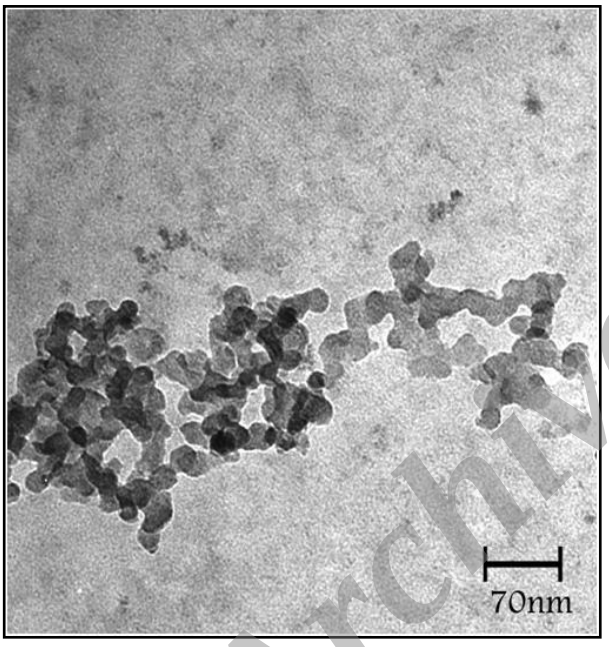

Fig. 4. Transmission electron microscopy (TEM) image of b ZnS/MCM-41.

CONCLUSIONS

In this paper, we have reported a simple method to synthesize ZnS nanoparticles in MCM-41 material hosts. A blue shift in the absorption edge was observed in the samples prepared by an ion-exchange method, indicating the formation of nanometer-sized ZnS nanoparticles in MCM-41 mesopore, as a consequence of particle size effects.

REFERENCES

[1] Pourahmad A., Sohrabnezhad Sh., Radaee E., (2010), Degradation of Basic Blue 9 dye by CoS/nanoAlMCM-41 catalyst under visible light irradiation. *J. Porous Mater.* 17: 367-375.

[2] Pourahmad A., Sohrabnezhad Sh., (2009), Preparation and characterization of Ag nanowires in mesoporous MCM-41 nanoparticles template by chemical reduction method. *J. Alloys Compd.* 484: 314-316.

[3] Pourahmad A., Sohrabnezhad Sh., Sadjadi, M.S., Zare K., (2008), Preparation and characterization of host (mesoporous aluminosilicate material) - guest (semiconductor nanoparticles) nanocomposite materials. *Mater. Lett.* 62: 655-658.

[4] Pourahmad A. Sohrabnezhad Sh., (2011), Synthesis and characterization of CoS nanoparticles encapsulated in mesoporous aluminosilicate material by solid-state reaction. *Mater. Lett.*, 65: 205-207.

[5] Kumbhojkar N., Nikesh V. V., Kshirsagar A., Mahamuni S., (2000), Photophysical properties of ZnS nanoclusters. *J. Appl. Phys.* 88: 6260-6264.

[6] Beck J. S., Vartuli C., Roth W. J., Leonowicz M. E., Kresge C. T., Scmmitt K. D., (1992), A new family of mesoporous molecular sieves prepared with liquid crystal templates. *J. Am. Chem. Soc.* 114: 10834-10843.

[7] Sohrabnezhad Sh., Pourahmad A., (2007), New Methylene Blue (NMB) Encapsulated in Mesoporous AlMCM-41 Material and Its Application for Amperometric determination of Ascorbic Acid in Real Samples. *Electroanal.* 15: 1635-1641.

[8] Sohrabnezhad Sh., Pourahmad A., Sadjadi M. S., Sadeghi B., (2008), Nickle cobalt

sulfide nanoparticles grown on AlMCM-41 molecular sieve. *Physica E*. 40: 684-688.

[9] Cai Q., Luo Zh-Sh., Pang W. Q., Fan Yu-W., Chen Xi-H., Cui Fu-Zh., (2001), Dilute solution routes to various controllable morphologies of MCM-41 silica with a basic medium. *Chem. Mater*. 13: 258-263.

[10] Flores-Acosta M., Sotelo-Lerma M., Arizpe-Charez H., Castillon-Barraza F. F., Ramirez-Bon R., (2003), Excitonic absorption of spherical PbS nanoparticles in zeolite A. *Solid State Commun.* 128: 407-411.

[11] Ochoa-Landin R., Flores-Acosta M., Ramirez-Bon R., Arizpe-Charez H., Sotelo-lerma M. & Castillon-Barraza F. F., (2003), Characterization of CdS clusters in zeolite A grown in alkalin solution. *J. Phys. Chem. Sol*. 64: 2245-2251.

[12] Sathish M., Viswanathan B. Viswanathan R. P., (2006), Alternate synthetic strategy for the preparation of CdS nanoparticles and its exploitation for water splitting. *Int. J. Hydrogen*. 31: 891-898.

[13] Wang Y. Herron N., (1987), Optical properties of cadmium sulfide and lead (II) sulfide clusters encapsulated in zeolites. *J. Phys. Chem.* 91: 257-260.

[14] Chen W., Wang Z. Lin L., (1997), Thermoluminescence of CdS clusters in zeolite-Y. *J. Luminescence*. 71: 51-156.

[15] Tandon S. P. Gupta J. P., (1970), Measurement of Forbidden Energy Gap of Semiconductors by Diffuse Reflectance Technique. *Phys. Status. Solidi*. 38: 363-367.

[16] Vossmeyer T., Katsikas L., Giersig M., Popovic I. G., Diesner K., Chemseddine A., Eychmuller A. Weller H., (1994), CdS nanoclusters synthesis, characterization, size dependent oscillator strength, temperature shift of the excitonic transition energy, and reversible absorbance shift. *J. Phys. Chem.* 98: 7665-7673.

[17] Sohn J. R., DeCanio S. J., Lunsford J. H. Odonnell D. J., (1986), Determination of framework aluminium content in dealuminated Y-type zeolites: a comparison based on unit cell size and wavenumber of i.r. bands. *Zeolites*. 6: 225-227.

[18] Umamaheswari V., Palanichamy M. Murugesan V., (2002), Isopropylation of m-Cresol over mesoporous Al-MCM-41 molecular sieves. *J. Catal*. 210: 367-374.

[19] Sun A. Sachtler W. M. H., (2003), Mn/MFI catalyzed reduction of NO_x with alkanes. *Appl. Catal. B*. 42: 393-401.

[20] Wellmann H., Rathousky J., Wark M., Zukal A. Schulz-Ekloff G., (2001), Structural investigation of Zinc Oxide clustering in zeolite A and sodalite. *Micropor. Mesopor. Mater*. 44: 419-425.

Cite this article as: A. Pourahmad: Ion exchange growth of Zinc Sulfide quantum dots in aqueous solution. ***Int. J.Nano Dimens.*** 6(1): 83-88, Winter 2015